



Project 3: Mean Field Methods for Bosons

Mione Filippo, Rigo Mauro, Slongo Francesco

April 28, 2020

University of Trento
Department of Physics
Via Sommarive, 14, 38123 Povo
Trento, Italy

Abstract

We studied the Gross-Pitaevskii equation. We implemented a self-consistent algorithm to calculate the ground state energy and wave function of bosons with a repulsive contact potential. We found that for small values of Na there is no need to mix the new and the previous potentials to reach convergence, while for larger Na small values of α are needed, which implies that the time for convergence is higher. Later we assessed which integration algorithm between Numerov and finite difference is the best and found that this depends on the conditions we choose. Lastly we studied the possibility of an attractive interaction and we obtained an instability of the system for $Na \leq -0.575$.

1 Introduction to the physical problem

The purpose of this report is to study the ground state of a system of interacting bosons and, in particular, estimate numerically the ground state energy and the ground state wave function.

We assume that the Hamiltonian of N identical bosons in coordinate space is

$$\hat{H} = \sum_{i=1}^N \left(-\frac{\hbar^2}{2m} \nabla_i^2 + v_{\text{ext}}(\mathbf{r}_i) \right) + \sum_{i<j}^N v(\mathbf{r}_i, \mathbf{r}_j) \quad (1)$$

where $v_{\text{ext}}(\mathbf{r}_i)$ is an external potential and $v(\mathbf{r}_i, \mathbf{r}_j)$ is the interaction potential between the bosons. Note that we have assumed the interaction to be only a 2-body force (that is, for example, we are not considering bosons that interact through the nuclear force).

We study the system in its ground state, at $T = 0$. The wave function of the system must satisfy the Schrödinger equation

$$\hat{H}|\Psi_0\rangle = E_0|\Psi_0\rangle \quad (2)$$

The main issue here is that $|\Psi_0\rangle$ cannot be determined explicitly.

To handle this issue, one can adopt a Mean Field approach, in which the interaction between the particles is replaced with an average interaction, equal for all particles. This way, since the particles are bosons, the wave function of the ground state is given by the product of identical single particle wave functions:

$$\Psi_0(\mathbf{r}_1, \dots, \mathbf{r}_N) = \prod_{i=1}^N \phi(\mathbf{r}_i) \quad (3)$$

Notice that the total wave function in this form is already symmetric under the exchange of 2 particles, as one should require for a wave function which describes bosons.

In order to estimate the ground state energy we use the variational method, with the constraint that the wave function must be normalised

$$\frac{\delta}{\delta\phi^*} \left(E[\phi] - \mu' \int_V |\phi(\mathbf{r})|^2 d\mathbf{r} \right) = 0 \quad (4)$$

where $E[\phi]$ is the energy functional and it depends on the single particle wave function $\phi(\mathbf{r})$. After some algebra one can obtain the expression

$$E[\phi] = T[\phi] + V_{\text{ext}}[\phi] + V_{\text{int}}[\phi] \quad (5)$$

where T is the kinetic term, V_{ext} is the external potential term and V_{int} is the interaction potential term:

$$\begin{aligned} T[\phi] &= N \int_V \phi^*(\mathbf{r}) \left(-\frac{\hbar^2}{2m} \nabla^2 \right) \phi(\mathbf{r}) d\mathbf{r} \\ V_{\text{ext}}[\phi] &= N \int_V |\phi(\mathbf{r})|^2 v_{\text{ext}}(\mathbf{r}) d\mathbf{r} \\ V_{\text{int}}[\phi] &= \frac{N(N-1)}{2} \int_V \int_V |\phi(\mathbf{r})|^2 |\phi(\mathbf{r}')|^2 v(\mathbf{r}, \mathbf{r}') d\mathbf{r} d\mathbf{r}' \end{aligned} \quad (6)$$

We notice that both $V_{\text{ext}}[\phi]$ and $V_{\text{int}}[\phi]$ depend only on the square modulus of ϕ ; this means that we could rewrite these terms as functions of the one-body density $\rho(\mathbf{r})$ only.

The one-body density operator is defined as

$$\hat{\rho}(\mathbf{r}) = \sum_{i=1}^N \delta(\mathbf{r} - \mathbf{r}_i) \quad (7)$$

and so

$$\langle \Psi_0 | \hat{\rho} | \Psi_0 \rangle = N |\phi(\mathbf{r})|^2 \equiv \rho(\mathbf{r}) \longrightarrow |\phi(\mathbf{r})|^2 = \frac{\rho(\mathbf{r})}{N} \quad (8)$$

This way the potential terms of the energy functional read

$$\begin{aligned} V_{\text{ext}}[\rho] &= \int_V \rho(\mathbf{r}) v_{\text{ext}}(\mathbf{r}) d\mathbf{r} \\ V_{\text{int}}[\rho] &= \frac{1}{2} \frac{N-1}{N} \int_V \rho(\mathbf{r}) \rho(\mathbf{r}') v(\mathbf{r}, \mathbf{r}') d\mathbf{r} \end{aligned} \quad (9)$$

Previously, we applied the variational method with the constraint that the single particle wave function must be normalized. Instead, we can require that the number of particles is kept constant:

$$\frac{\delta}{\delta \phi^*} \left(E[\phi] - \mu \int_V \rho(\mathbf{r}) d\mathbf{r} \right) = 0 \quad (10)$$

where $\mu = \mu'/N$. It can be thus shown that performing the minimization yields:

$$\left(-\frac{\hbar^2}{2m} \nabla^2 + v_{\text{ext}}(\mathbf{r}) + \frac{N-1}{N} \int_V \rho(\mathbf{r}') v(\mathbf{r}, \mathbf{r}') d\mathbf{r}' \right) \phi(\mathbf{r}) = \mu \phi(\mathbf{r}) \quad (11)$$

This equation is called *Hartree equation* and the third term in the parentheses is the *Hartree term*, a potential like term that depends on the wave function itself. Notice that we started from the SE, which is a linear differential equation, and obtained a non-linear differential equation. It is important to observe that μ is *not* the single particle energy of the ground state; in fact, multiplying Eq. (11) by $N\phi(\mathbf{r})^*$ and integrating in $d\mathbf{r}$ gives

$$N\mu = T[\phi] + V_{\text{ext}}[\phi] + 2V_{\text{int}}[\phi] \quad \Rightarrow \quad E_\mu[\phi] = N\mu - V_{\text{int}}[\phi] \quad (12)$$

Note that we used $E_\mu[\phi]$ rather than $E[\phi]$; these two functionals are clearly equal if ϕ is indeed the solution of Eq. (11). However, we shall see that, due to the procedure used to solve the equation, $E_\mu[\phi]$ and $E[\phi]$ are not equal unless ϕ has converged to the correct solution.

We focus our attention on a system of ultracold bosonic atoms trapped by a laser and we approximate v_{ext} to an harmonic potential. For simplicity, we consider a very diluted system, which should not feature strong long range interactions. Moreover, at first order¹, we can approximate the short-range interaction

¹The contact potential is the first order expansion of the interaction potential in the momentum transfer, which we assume to be low by considering a low density.

with a contact potential that represents the core impenetrability of the particles. The contact potential reads

$$v_{\text{int}}(\mathbf{r}, \mathbf{r}') = \frac{4\pi\hbar^2 a}{m} \delta(\mathbf{r} - \mathbf{r}') \quad (13)$$

where a is the scattering length (the only physically relevant quantity). With these previous hypotheses, the Hartree equation becomes

$$\left(-\frac{\hbar^2}{2m} \nabla^2 + \frac{m\omega^2 r^2}{2} + \frac{4\pi\hbar^2 a(N-1)}{mN} \int_V \rho(\mathbf{r}) \delta(\mathbf{r} - \mathbf{r}') d\mathbf{r}' \right) \phi(\mathbf{r}) = \mu \phi(\mathbf{r}) \quad (14)$$

Now we can also assume $N \gg 1$ and that the ground state is rotationally invariant. The former hypothesis implies $(N-1)/N \simeq 1$, while the latter allows to write

$$\phi(\mathbf{r}) = \frac{R_{0,0}(r)}{r} \frac{1}{\sqrt{4\pi}} \quad (15)$$

We can thus recast the Hartree equation in the following form:

$$\left(-\frac{\hbar^2}{2m} \frac{d^2}{dr^2} + \frac{m\omega^2 r^2}{2} + \frac{Na\hbar^2}{m} \int_0^\infty \left[\frac{R(r')}{r'} \right]^2 \delta(r - r') dr' \right) R(r) = \mu R(r) \quad (16)$$

We can also rescale the problem using the harmonic oscillator length $a_{\text{HO}} = \sqrt{\hbar/(m\omega)}$ and $\tilde{r} = r/a_{\text{HO}}$ to get

$$\left[-\frac{\hbar\omega}{2} \frac{d^2}{d\tilde{r}^2} + \frac{\hbar\omega\tilde{r}^2}{2} + \hbar\omega N\tilde{a} \left(\frac{R(\tilde{r})}{\tilde{r}} \right)^2 \right] R(\tilde{r}) = \mu R(\tilde{r}) \quad (17)$$

where $\tilde{a} = a/a_{\text{HO}}$. Finally, if we divide the equation by $\hbar\omega$ and use proper units for μ , we obtain the so called *Gross-Pitaevskii equation*:

$$\left[-\frac{1}{2} \frac{d^2}{d\tilde{r}^2} + \frac{\tilde{r}^2}{2} + N\tilde{a} \left(\frac{R(\tilde{r})}{\tilde{r}} \right)^2 \right] R(\tilde{r}) = \mu R(\tilde{r}) \quad (18)$$

To avoid clunky notation, from now on we shall drop the tildes and use r and a in units of oscillator length, unless stated otherwise.

2 Introduction to the computational problem

To solve numerically the Gross-Pitaevskii equation (Eq. (18)), it is convenient to use suitable measurement units in order to deal with quantities close to unit and avoid inconsistent results due to a computer's internal representation of floating point numbers. As the equation itself suggests, we set the harmonic oscillator length a_{HO} and $\hbar\omega$ to 1.

Solving Eq. (18) involves multiple issues. To begin with, the eigenvalue μ is not known a priori. Moreover, the Hartree term $Na(R(r)/r)^2$ depends on the solution itself (making Eq. (18) a *self consistent* equation) and therefore it is not possible to use an algorithm that solves a simple differential equation.

The latter problem is solved with an iterative procedure, which begins by proposing a reasonable ground state wave function $R^{(0)}(r)$. Then one calculates the corresponding Hartree potential $Na(R^{(0)}(r)/r)^2$ and plugs the result into Eq. (18). Now (assuming μ is known) it is possible to integrate the second order differential equation with any numerical method and, by doing it, one obtains a new wave function $R^{(1)}(r)$. Unless the guessed $R^{(0)}(r)$ is the correct ground state wave function, one has $R^{(1)}(r) \neq R^{(0)}(r)$. This procedure is then repeated until convergence. In general it is not a wise choice to use $R^{(i)}(r) \simeq R^{(i+1)}(r)$ as stopping criterion, because often this is a non stable condition. Instead,

we can exploit the aforementioned fact that $E[\phi] \neq E_\mu[\phi]$ unless R (and therefore ϕ) is the correct, converged solution. Thus we can calculate the difference $|E[\phi] - E_\mu[\phi]|$ and repeat the procedure until this difference is smaller than an arbitrary threshold ε . In the case of the Gross-Pitaevskii equation, it is more convenient to use the single particle functionals² $T[\phi]$, $V_{\text{ext}}[\phi]$ and $V_{\text{int}}[\phi]$:

$$\begin{aligned} T[\phi] &= T[R] = -\frac{1}{2} \int_V R(r) \frac{\partial^2}{\partial r^2} R(r) dr \\ V_{\text{ext}}[\phi] &= V_{\text{ext}}[R] = \frac{1}{2} \int_V r^2 |R(r)|^2 dr \\ V_{\text{int}}[\phi] &= V_{\text{int}}[R] = \frac{Na}{2} \int_V \frac{|R(r)|^4}{r^2} dr \end{aligned} \quad (19)$$

and with these definitions the single particle energy functionals that we shall employ in the check for convergence are $E[\phi] = T[\phi] + V_{\text{ext}}[\phi] + V_{\text{int}}[\phi]$ and $E_\mu[\phi] = \mu - V_{\text{int}}[\phi]$. To evaluate the integrals, we use the Cavalieri-Simpson algorithm, which has an error $O(h^4)$, where h is the mesh step. While the integration of $V_{\text{ext}}[\phi]$ and $V_{\text{int}}[\phi]$ entails no additional calculations, for $T[\phi]$ we need to calculate the second order derivative of the wave function $R(r)$. To have an error of the same order of the one associated with the Cavalieri-Simpson algorithm, we estimate the second derivative with a 5 points formula:

$$\frac{\partial^2}{\partial r^2} R(r) = \frac{1}{12h^2} [-30R(r) + 16R(r+h) + 16R(r-h) - R(r+2h) - R(r-2h)] + O(h^4) \quad (20)$$

Of course, we cannot use this expression at the extrema (as well as the points immediately adjacent to them) of the integration range. Obtaining a formula for the second derivative at an extremum of a mesh with $O(h^4)$ error is rather easy, and one can check that at the first and second points of the mesh the following formula can be employed:

$$\begin{aligned} \frac{\partial^2}{\partial r^2} R(r) &= \frac{1}{12h^2} [45R(r) - 154R(r+h) + 214R(r+2h) \\ &\quad - 156R(r+3h) + 61R(r+4h) - 10R(r+5h)] + O(h^4) \end{aligned} \quad (21)$$

At the upper extremum and the point before it we can use the same formula, just with minus signs instead of plus signs inside the argument of R . To normalize the wave functions we use the Simpson algorithm as well.

Additionally, another problem that one may encounter lies in the fact that the solution could not directly converge to the correct solution, rather it could oscillate around it (e.g. there may be situations in which $R^{(i+1)}(r) \neq R^{(i)}(r)$ and $R^{(i+2)}(r) \simeq R^{(i)}(r)$, and the solutions keep bouncing from one expression to the other without reaching the correct one). To handle this problem it is customary to calculate the Hartree potential not directly using $R^{(i)}(r)$, but from a mixture of the new density calculated using $R^{(i)}(r)$ and the one used in the previous self-consistent step, i.e.

$$\rho_{\text{H}}^{(i)} = \alpha \rho^{(i)} + (1 - \alpha) \rho_{\text{H}}^{(i-1)} \quad (22)$$

where $\rho^{(i)} = (R^{(i)})^2$ and ρ_{H}^i is the density to be used for the Hartree potential in the i -th iteration of the self consistent procedure. For $\alpha = 1$ the procedure is equivalent to that described above. On the contrary, if α is small, the Hartree potential doesn't change too much³ from one iteration to the other and therefore the wave function doesn't change too much either, so the convergence to the true wave

²These are just the functionals previously introduced divided by N , though we use the same names for ease of notation; from this point on we shall use this notation to indicate only the single particle functionals.

³With "too much" we are purposefully being vague, because, as we shall see in the next section, the optimal value of α as well as the optimal variation in the Hartree potential depend on the potential itself.

function can be more accurate. Of course, the smaller α is the closer the solutions will oscillate to the true solution, but at the same time the slower the algorithm will converge.

Finally, to integrate the Gross-Pitaevskii equation at one given iteration of the self consistent procedure we use the Numerov algorithm and a finite difference method. The details concerning the Numerov algorithm have already been discussed in our first work; here we shall limit ourselves to a brief summary. Let us consider a linear and homogeneous second order differential equation

$$\frac{d^2 y(r)}{dr^2} + k^2(r)y(r) = 0 \quad (23)$$

To solve this numerically, we first discretize the coordinate interval into a mesh $\{r_0, r_1, \dots, r_{N-1}\}$ with mesh step $r_{i+1} - r_i = h$. The Numerov algorithm calculates y at the point r_{i+1} as

$$y_{i+1} = \frac{y_i \left(2 - \frac{5}{6} h^2 k_i^2\right) - y_{i-1} \left(1 + \frac{h^2}{12} k_{i-1}^2\right)}{1 + \frac{h^2}{12} k_{i+1}^2} \quad (24)$$

In the case of the Gross-Pitaevskii equation y corresponds to $R(r)$, while $k^2(r)$ to

$$k^2(r) = 2 \left[\mu - \frac{1}{2} r^2 - Na \frac{\rho(r)}{r^2} \right] \quad (25)$$

To find μ we use the false position method.

As for the finite difference method, once again we discretize the coordinate interval; this time, though, instead of evolving the wave function, the problem is recast into a linear eigenvalues problem. Let us consider the discretized version of Eq. (18) and expand the derivative with a 3 point method:

$$-\frac{1}{2} \frac{R_{i+1} - 2R_i + R_{i-1}}{h^2} + \mathcal{O}(h^2) + \frac{r_i^2}{2} R_i + Na \frac{\rho_i}{r_i^2} R_i = \mu R_i \quad (26)$$

If we define

$$U_i = \frac{1}{h^2} + \frac{r_i^2}{2} + Na \frac{\rho_i}{r_i^2} \quad (27)$$

we have that

$$UR = \mu R \rightarrow \begin{pmatrix} U_1 & -\frac{1}{2h^2} & 0 & \cdots & 0 & 0 \\ -\frac{1}{2h^2} & U_2 & -\frac{1}{2h^2} & \cdots & 0 & 0 \\ 0 & -\frac{1}{2h^2} & U_3 & \cdots & 0 & 0 \\ \vdots & \vdots & \vdots & \ddots & \vdots & \vdots \\ 0 & 0 & 0 & \cdots & U_{N-2} & -\frac{1}{2h^2} \\ 0 & 0 & 0 & \cdots & -\frac{1}{2h^2} & U_{N-1} \end{pmatrix} \begin{pmatrix} R_1 \\ R_2 \\ R_3 \\ \vdots \\ R_{N-2} \\ R_{N-1} \end{pmatrix} = \mu \begin{pmatrix} R_1 \\ R_2 \\ R_3 \\ \vdots \\ R_{N-2} \\ R_{N-1} \end{pmatrix} \quad (28)$$

where we have taken into account the fact that $R_0 = 0$ and assumed that $R_N = 0$ (equivalently, we imposed $V(r) = \infty$ for $r \geq r_N$). To solve the eigenvalue problem we can use suitable subroutines of different libraries (GSL, Eigen, ALGLIB, ...).

3 Discussion

3.1 Point 1

Sec. (2) describes in detail the procedure employed to solve the Gross-Pitaevski equation. This method is actually more general and can be applied to other mean field approaches, when the result is a self-consistent equation of the following form

$$-\frac{\hbar^2}{2m}\nabla^2\phi_\alpha(\mathbf{r}) + v_{\text{ext}}(\mathbf{r})\phi_\alpha(\mathbf{r}) + U_{\text{eff}}(\rho(\mathbf{r}))\phi_\alpha(\mathbf{r}) = \mu_\alpha\phi_\alpha(\mathbf{r}) \quad (29)$$

A general approach to deal with self consistent equations is pictured in the flowchart in Fig. 1.

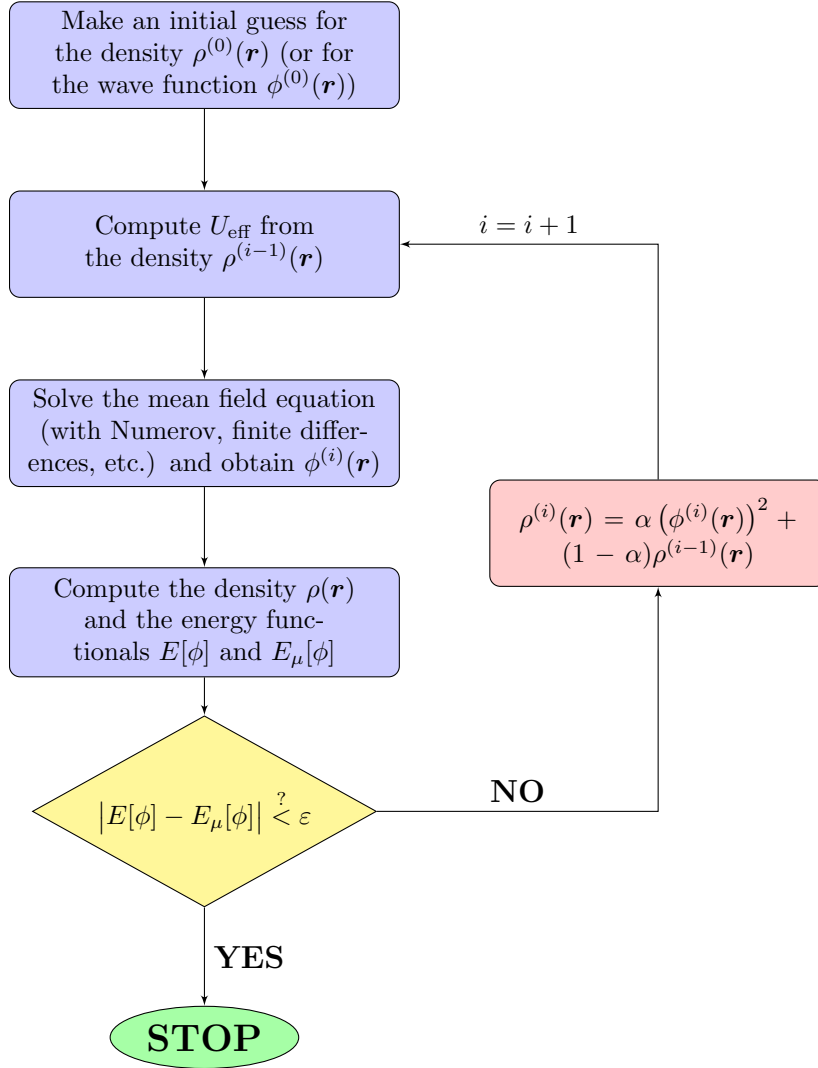


Figure 1: Flow chart of an algorithm to solve mean field problems which involve a self consistent equation.

3.2 Point 2

Before actually solving Eq. (18) with the method outlined in Sec. (2) and pictured in Fig. 1, we first test only one iteration of the algorithm (with the Hartree potential calculated as $Na\alpha (R_{\text{HO}}(r)/r)^2$, that is Eq. (22) with $\rho_{\text{H}}^{(i-1)} = 0$ and the 3D harmonic oscillator ground state as guess for the initial wave function) to see how the parameters Na and α influence the wave function and the ground state energy.

We run one iteration of the algorithm for $Na = 0.01, 1, 100$ and $\alpha = 0.01, 0.1, 0.5, 1.0$ using $h = 10^{-3}$ and $r_{\max} = 7$, the results are in Figs 2, 3 and 4.

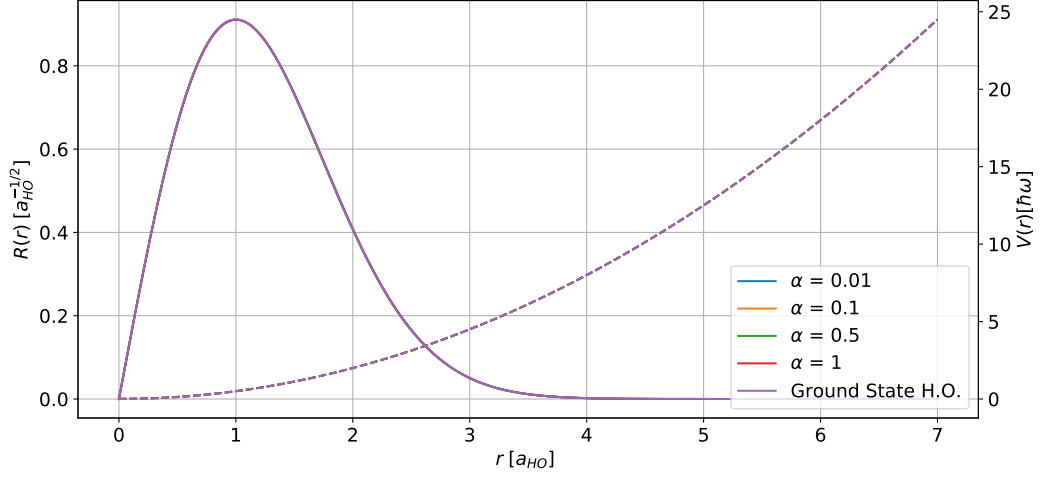


Figure 2: Plot of the wave functions (continuous line) and the relative potentials (dashed line) for $Na = 0.01$. Functions not visible are overlapped to the ground state of the harmonic oscillator. Notice that the potential is referred to the y axis on the right.

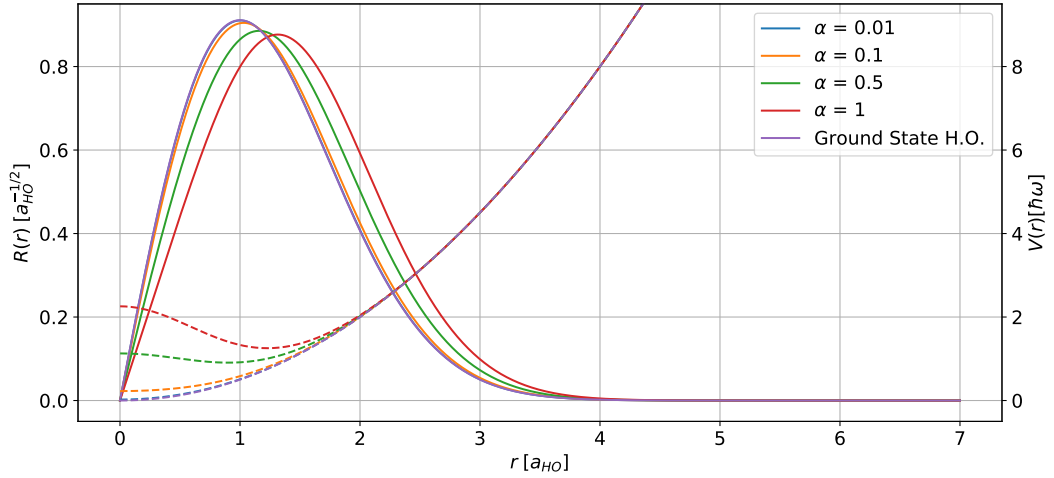


Figure 3: Plot of the wave functions (continuous line) and the relative potentials (dashed line) for $Na = 1$. Functions not visible are overlapped to the ground state of the harmonic oscillator. Notice that the potential is referred to the y axis on the right.

One can immediately notice that for $Na = 0.01$ there is not a visible departure both from the H.O. ground state and its potential. On the contrary, the last two pictures show the presence of a hump at the origin; this is of course expected, because the initial guess of the wave function is a Gaussian multiplied by r , so the Hartree potential becomes a simple Gaussian. This explains the reason why the wave function shifts towards higher values of r and also the fact that the higher $Na\alpha$ is the more the wave functions moves the right.

The wave functions for high values of $Na\alpha$ display a peculiar behaviour close to the origin. While the H.O. ground state is proportional to r for small values of r and this seems to be the case also for small

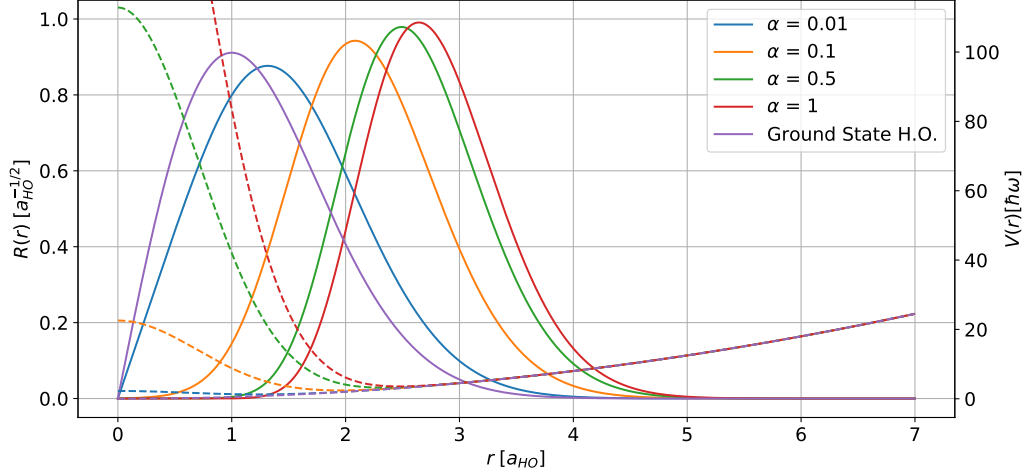


Figure 4: Plot of the wave functions (continuous line) and the relative potentials (dashed line) for $Na = 100$. Functions not visible are overlapped to the ground state of the harmonic oscillator. Notice that the potential is referred to the y axis on the right. We choose not to include the whole curve of the potential for $\alpha = 1$ at the origin since it would cause the others to become rather indistinguishable. Note that, as explained above, its behaviour is simply that of a Gaussian for small r .

values of $Na\alpha$ (Fig. 3), as one can see from Fig. 4 the wave function for big $Na\alpha$ assumes a form that resembles more a shifted Gaussian. This may be due to the fact that, when $Na\alpha$ is small, the energy of the bound state is higher or close to the value of the potential at $r = 0$, whereas for big values of $Na\alpha$ the energy of the bound state is significantly lower than the potential at $r = 0$ and the wave function yields a very low probability density for $r \rightarrow 0$.

Finally we study the values of μ and of the functionals $T[\phi]$, $V_{\text{ext}}[\phi]$, $V_{\text{int}}[\phi]$, $E[\phi]$ and $E_{\mu}[\phi]$ obtained after one iteration: the results are in Tab. 1. For completeness, we also report the value of the potential at the first point of the mesh ($r_0 = h$) $V_{\text{tot}}(h)$ to allow a comparison with the energy eigenvalue of the state μ .

	α	μ [$\hbar\omega$]	$T[\phi]$ [$\hbar\omega$]	$V_{\text{ext}}[\phi]$ [$\hbar\omega$]	$V_{\text{int}}[\phi]$ [$\hbar\omega$]	$E_{\mu}[\phi]$ [$\hbar\omega$]	$E[\phi]$ [$\hbar\omega$]	$V_{\text{tot}}(h)$ [$\hbar\omega$]
$Na = 0.01$	0.01	1.50008	0.74997	0.75003	0.00398914	1.49609	1.50399	0.0002277
	0.1	1.5008	0.749701	0.750299	0.00398657	1.49681	1.50399	0.0022588
	0.5	1.50399	0.748506	0.751497	0.00397519	1.50001	1.50398	0.0112857
	1	1.50796	0.747017	0.752997	0.003961	1.504	1.50398	0.0225695
$Na = 1$	0.01	1.50796	0.747017	0.752997	0.3961	1.11186	1.89611	0.0225695
	0.1	1.57836	0.721018	0.780409	0.371414	1.20695	1.87284	0.225678
	0.5	1.8635	0.62483	0.91007	0.28081	1.58269	1.81571	1.12838
	1	2.15947	0.548857	1.08073	0.206184	1.95328	1.83577	2.25675
$Na = 100$	0.01	2.15947	0.548857	1.08073	20.6184	-18.4589	22.248	2.25675
	0.1	3.71716	0.629251	2.41067	7.50297	-3.78581	10.5429	22.5676
	0.5	4.77324	0.751236	3.3825	5.51701	-0.743773	9.65075	112.837
	1	5.21279	0.79473	3.7889	4.99218	0.22061	9.57581	225.675

Table 1: Values of μ and of the functionals for different Na and α .

From Tab. 1 we can see that μ increases as α and Na increase and, as expected, it is constant for $Na\alpha$ constant. At small $Na\alpha$ $T[\phi]$ and $V_{\text{ext}}[\phi]$ are very similar between each other (and close to

$3/4\hbar\omega$); in fact, in these conditions the potential is very close to that of the harmonic oscillator, for which one expects these functionals to be equal (as from the Virial theorem). For constant $Na\alpha$, the only functional that differs from one α to the other is $V_{\text{int}}[\phi]$, which is to be expected given the definition of the Hartree potential. Moreover, we can also observe the effect of the shift of the maximum of the wavefunction towards high values of r at high $Na\alpha$ in the fact that V_{ext} increases as this parameter increases. Additionally, it is interesting to notice that $E_{\mu}[\phi]$ can assume negative values, which is clearly not physical for a potential that is always positive. Finally one can observe that the discrepancy between $E[\phi]$ and $E_{\mu}[\phi]$ is larger for higher Na . This is reasonable, since for small Na the potential is close to the harmonic oscillator and the first guess for the wave function is the ground state of the harmonic oscillator. For large Na the potential becomes significantly different from the harmonic oscillator potential, which explains the higher difference in the energy functionals.

3.3 Point 3

In this section we consider the full solution of the Gross-Pitaevskii equation with the self consistent procedure for $Na = 0.01, 0.1, 1, 10, 100$. As described in Sec. 2, we introduce a mixing parameter α to guarantee convergence; in fact, as shown in the previous section, the bigger the value of α the higher the discrepancy between wave functions of successive iterations, which could cause the algorithm not to succeed in finding the solution. As mentioned above, as a criterion to determine the convergence of the algorithm we use the difference between the energy functionals $|E[\phi] - E_{\mu}[\phi]|$, where all the functionals (kinetic energy, external potential and interaction potential) are calculated as explained in Sec. 2. It is important to notice that one usually fixes a threshold E_t for the energy functionals difference and considers the solution to "converge" when $|E[\phi] - E_{\mu}[\phi]| < E_t$, though for the sake of generality throughout this and the next sections we shall let this value reach the minimum allowed by numerical errors and, in that case, consider the procedure to "converge". Note that, for high thresholds, there may be values of α that lead to a (slightly) faster convergence, though the α we consider "optimal"⁴ is more general and gives reasonably fast convergence for all thresholds within the range allowed by numerical error. Moreover, if for a given threshold a certain α yields the fastest convergence, for a lower threshold the procedure with the same α could not converge at all. Thus, here we consider "converging" only the cases in which in principle we could actually reach the minimum precision allowed by numerical errors.

In this section we only use the Numerov algorithm, setting a mesh step $h = 0.002$ which is a very favorable choice both in terms of accuracy and computational time, as we shall see in the next section. As a threshold for the false position method we use $E_t = 10^{-13}$ and as a last point in the mesh we used $r_{\text{max}} = 8$ for $Na = 100$ and $r_{\text{max}} = 6$ otherwise.

We began by considering $Na = 100$, seeking the optimal value of α in order to reach convergence. The result is summarized in Fig. 5, where we plot $|E[\phi] - E_{\mu}[\phi]|$ against the first 400 self consistent iterations for some of the tested values of α . As we shall see in the next section, fluctuations of the energy functionals difference around the minimum are due both to loss of numerical precision and by the intrinsic errors in the algorithms used; in fact, the errors of both the Numerov algorithm used to integrate the wave function and the Simpson integration rule which we employ to calculate the functionals are $O(h^4) \simeq 10^{-11}$ in this instance.

One can notice that the optimal value for α is $\alpha_0 = 0.09$, as it gives the fastest convergence to the minimum energy difference, which is indeed of order 10^{-11} . Fig. 5 also shows that for high values of α the algorithm doesn't reach convergence, rather it stabilizes around a high value and oscillates between two different wave functions. On the contrary, for values of $\alpha < \alpha_0$ the algorithm still converges but takes a higher number of iterations.

⁴Note, however, that we didn't employ a proper analytic minimization.

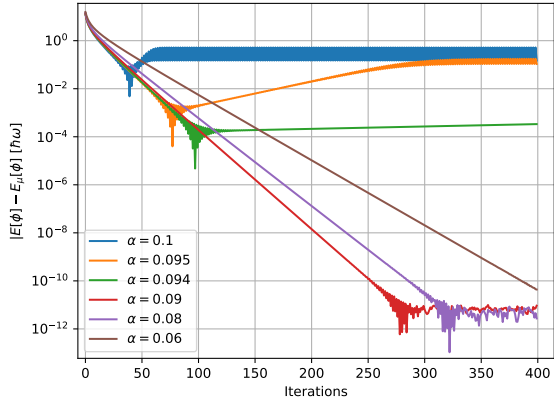


Figure 5: Energy functionals difference as a function of the number of iterations for $Na = 100$.

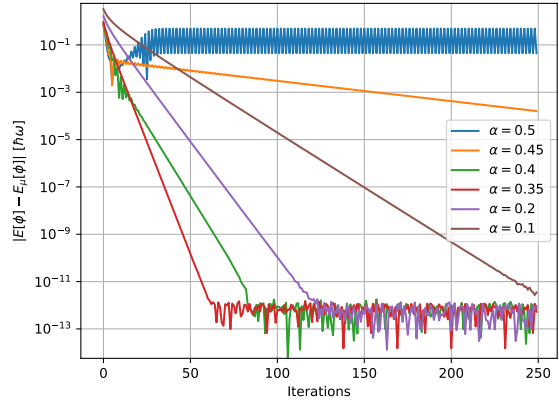


Figure 6: Energy functionals difference as a function of the number of iterations for $Na = 10$.

The same considerations can be done for the case $Na = 10$, which we analyze in Fig. 6. Here we see that the optimal value is $\alpha_0 = 0.35$ and the energy functionals difference converges much more quickly than the $Na = 100$ case, which is expected due to the need of using a lower value of α in the latter case. An interesting behaviour emerges from the case $\alpha = 0.45$, which shows the existence of values of $\alpha > \alpha_0$ for which the difference of the energy functionals initially decreases, then oscillates and decreases again with a different slope until convergence (not shown in the plot for the sake of clarity). These cases are in a sense half way between the convergent and the non convergent cases. The slope-changing behaviour is actually present for non converging curves as well, as shown in Fig. 5. We chose not to investigate the reason for this behaviour.

The case $Na = 1$, portrayed in Fig. 7, shows that every (tested) value of $\alpha \in (0, 1]$ leads to convergence, including $\alpha = 1$, for which we are no longer mixing the potentials but instead we substitute at each iteration the interaction potential evaluated using wave function at the previous step only. Nevertheless, we can still see that the optimal value is $\alpha_0 = 0.8$.

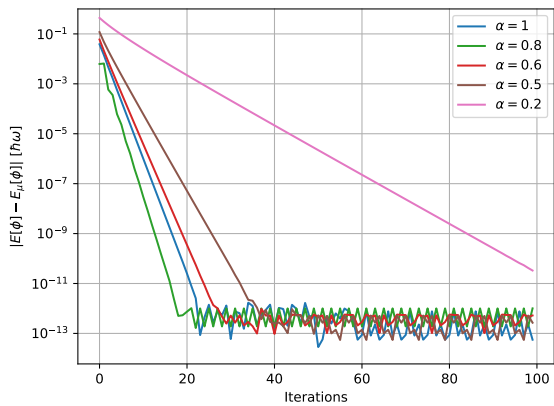


Figure 7: Energy functionals difference as a function of the number of iterations for $Na = 1$.

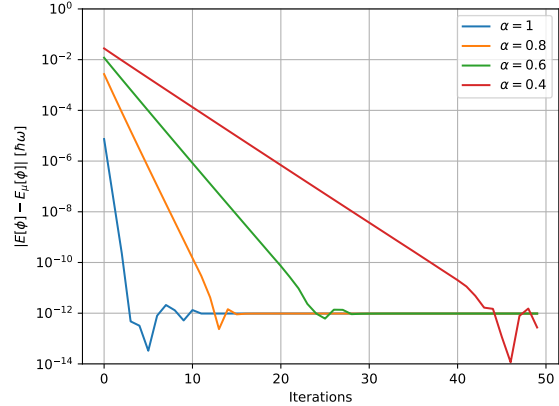


Figure 8: Energy functionals difference as a function of the number of iterations for $Na = 0.1$.

The cases of $Na = 0.1, 0.01$, which are illustrated in Figs 8 and 9, are rather similar: for both values of Na the procedure converges for every (tested) $\alpha \in (0, 1]$. As opposed to the previous case, here $\alpha = 1$ is the optimal parameter.

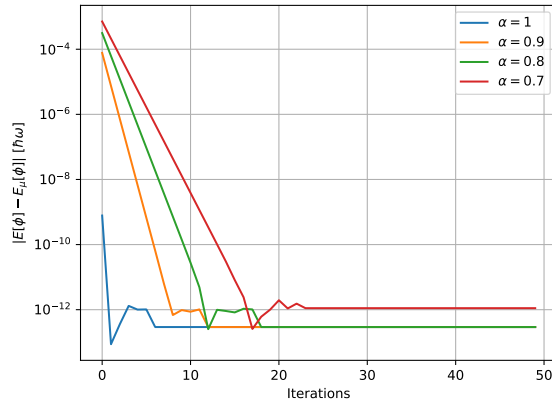


Figure 9: Energy functionals difference as a function of the number of iterations for $Na = 0.01$.

To give a brief summary of the results, we find that each value of Na has an associated optimal mixing parameter α_0 , all of which are reported in Tab. 2 alongside the energy to which the procedures converge. For $\alpha < \alpha_0$ the procedure converges as well, though in a larger number of iterations, while for $\alpha > \alpha_0$ in some cases the procedure converges whereas in other it doesn't. In some cases the behaviour of $|E[\phi] - E_\mu[\phi]|$ appears to change for high α at a number of iterations which decreases as α increases, reaching a slope which increases as α does so (this is one of the reasons why we chose the more general approach to convergence). We observe that the higher the value of Na the lower the α_0 , which is to be expected: in fact, Na quantifies the strength of the Hartree potential and, as already mentioned, in order to converge the potential needs to change only slightly between iterations, thus the mixing parameter has to change accordingly, taking smaller values for large Na . For small values of Na , the harmonic potential is very similar to the mean field potential at convergence, therefore every α leads to convergence and values closer to 1 yield a faster convergence rate.

Na	Optimal α	$E [\hbar\omega]$	N_{conv}
100	0.09	6.875	300
10	0.35	3.072	70
1	0.8	1.811	30
0.1	1	1.539	10
0.01	1	1.504	6

Table 2: Optimal values of α , final energy and number of steps to reach convergence for different values of Na .

Finally, the wave functions obtained at convergence alongside the respective mean field potential and the non interacting case (harmonic oscillator) are shown in Fig. 10. We observe that for bigger Na the wave functions are broader than the non interacting case: from a physical standpoint, this can be explained by the fact that we introduce a repulsive potential, therefore the stronger Na the higher the probability of finding particles at larger values of r . As for the potentials, as expected near the origin they are higher for larger Na , while away from the origin the harmonic oscillator term is dominant.

In the next section we shall consider the possibility of fixing an arbitrary energy functionals difference threshold to compare the Numerov algorithm with a finite difference one.

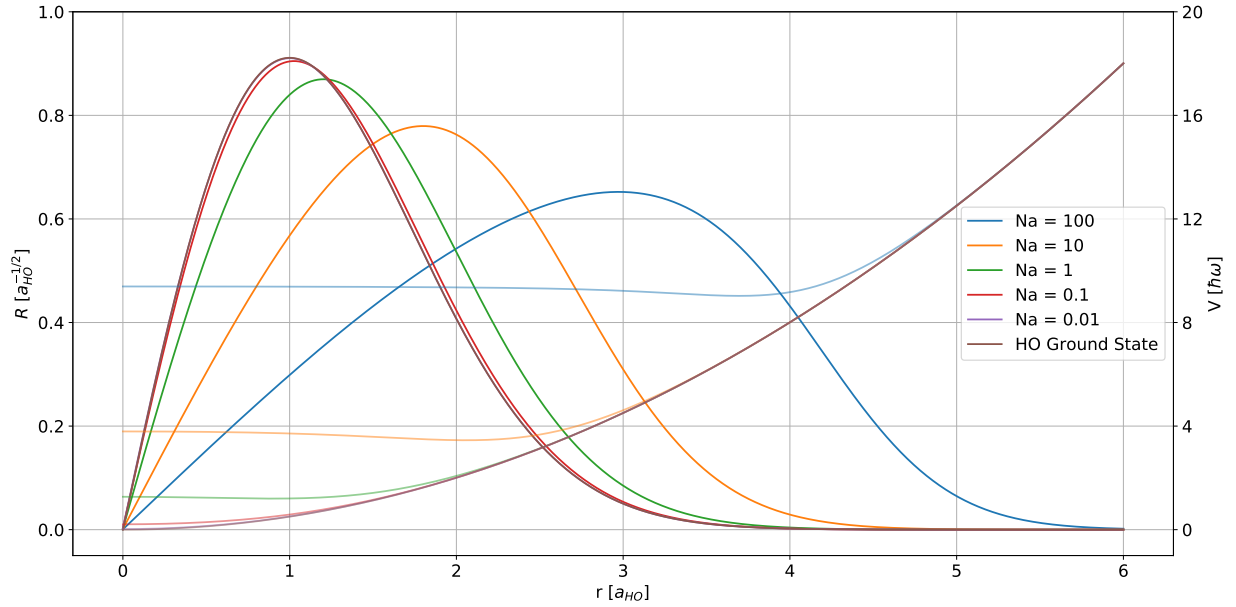


Figure 10: Results of the self consistent procedure for the Gross Pitaevskii equation for different values of the parameter Na . The resulting wave functions are plotted in a solid line and the corresponding mean field potentials in an transparent line of the same color. The H.O. ground state is the solution to the problem in the non interacting particle case ($Na = 0$). Notice that the potential is referred to the y axis on the right.

3.4 Point 4

In this section we study the same problem using a finite difference method (FD). The main issue with this method is that the dimension of the matrix to diagonalize scales with $N^2 = h^{-2}$ and, already with e.g. $h = 10^{-3}$ and $r_{\max} = 6$ one would need to allocate and diagonalize a 6000×6000 matrix. We tested various different subroutines of different libraries, namely `gsl_eigen_symmv` of `GSL`, the class `SelfAdjointEigenSolver` of `Eigen` and `smatrixtdevd` of `ALGLIB`. The first two are general symmetric matrices eigensolvers, while the last, imported from the `LAPACK` library for `FORTRAN`, is specifically written for symmetric tridiagonal matrices. There are other diagonalization subroutines (e.g. `tqli`) and libraries (e.g. `armadillo`) that we could use, though we choose to only test those mentioned above.

Since we are actually only interested in the lowest eigenvalue and the corresponding eigenvector, we could also use the subroutine `smatrixtdevdi` of `ALGLIB`, which allow to find tridiagonal matrix eigenvalues/vectors with given indexes by using the bisection and inverse iteration⁵; however, we decided to implement our own algorithm anyway, which actually proved to be more efficient than this subroutine (and much more than the others) and equally accurate in the compared cases.

In our implementation, we find the lowest eigenvalue by seeking the smallest zero of the characteristic polynomial of the matrix \mathbf{U} of Eq. (28) using the false position method. The characteristic polynomial is defined as

$$p(\lambda) = \det(\mathbf{U} - \lambda \mathbb{1})$$

To compute the determinant one could use the LU decomposition, though there also exists a simple

⁵As reported in the `ALGLIB` manual.

recursive $\mathcal{O}(N-1)$ relation for the tridiagonal $(N-1) \times (N-1)$ matrix of our interest: defining

$$f_n = \det [2h^2 (\mathbf{U}_n - \lambda \mathbf{1}_n)] = \det \begin{pmatrix} 2h^2(U_1 - \lambda) & -1 & \cdots & 0 & 0 \\ -1 & 2h^2(U_2 - \lambda) & \cdots & 0 & 0 \\ \vdots & \vdots & \ddots & \vdots & \vdots \\ 0 & 0 & \cdots & 2h^2(U_{n-1} - \lambda) & -1 \\ 0 & 0 & \cdots & -1 & 2h^2(U_n - \lambda) \end{pmatrix}$$

where $n = 1, \dots, N-1$ and $f_0 = 1, f_{-1} = 0$, we have

$$f_n = 2h^2(U_n - \lambda)f_{n-1} - (-1)(-1)f_{n-2}$$

and $p(\lambda) \propto f_{N-1}$. The proportionality constant only depends on h and can be neglected, since only the zeros of $p(\lambda)$ are relevant as far as the problem is concerned. Computing the determinant of $2h^2 (\mathbf{U}_n - \lambda \mathbf{1}_n)$ rather than $\mathbf{U}_n - \lambda \mathbf{1}_n$ allows to deal with smaller quantities (and avoid overflow errors).

Once the zero of $p(\lambda)$, $\lambda_0 = \mu$, is found, obtaining the eigenvector associated with μ translates into solving a linear system of equations

$$(\mathbf{U} - \mu \mathbf{1})\mathbf{R} = \mathbf{0} \quad \rightarrow \quad \mathbf{A}\mathbf{R} = \mathbf{0} \quad (30)$$

where once again we conveniently choose to multiply the equation by $2h^2$, that is $\mathbf{A} = 2h^2(\mathbf{U} - \mu \mathbf{1})$. Of course, the system is homogeneous and, assuming μ really is an eigenvalue of \mathbf{U} , the determinant of \mathbf{A} is null, thus we still have the freedom to arbitrarily choose one value of the wave function \mathbf{R} . We considered two alternatives to handle the issue. Since the matrix is symmetric and tridiagonal, one can easily find an iterative procedure to calculate the solution of the linear system, namely, fixing R_{N-1} to a small nonzero value ($R_N = 0$)

$$R_{i-1} = 2h^2(U_i - \mu)R_i - R_{i+1}$$

Fixing the last point of the mesh rather than the first is convenient in that, in the other case, the error accumulated by the procedure would lead to an early divergence of the wavefunction, while in this way the error mainly affects regions where the wavefunction is large⁶.

Since this procedure may involve a significant propagation of the error, we also considered leaving the task of solving the linear system to the GSL routine `gsl_linalg_solve_symm_tridiag`, specifically designed to solve tridiagonal symmetric systems, in the hope of obtaining more accurate results. However, using the GSL subroutine with Eq. (30) yields a solution which is identically zero. To deal with a non-homogeneous system instead of a homogeneous one, we can exploit the fact that, in principle, $R_0 = R(r=0) = 0$ and add to the system the equation $R_0 - R_1 = -h$. If R_0 is truly null, this condition would result in $R_1 = h$ and the second equation $-R_0 + 2h^2(U_1 - \lambda)R_1 - R_2 = 0$ would become the original $2h^2(U_1 - \lambda)R_1 - R_2 = 0$. This way, though, the vector on the right of Eq. (30) is not identically zero anymore and `gsl_linalg_solve_symm_tridiag` can yield a $\mathbf{R} \neq \mathbf{0}$. We shall refer to the former implementation as FD (1) and the latter as FD (2). In Tab. 3 we compare the results of the different algorithms for the ground state of the harmonic oscillator with different mesh steps. In particular, we study the accuracy on the true energy and wave function, the latter calculated as $\varepsilon = 1 - |\langle R_t | R_n \rangle|^2$ where R_t is the true ground state and R_n the numerical approximation. We used 10^{-13} as eigenvalue thresholds for our algorithms and $R_{N-1} = 10^{-20}$ for the first implementation.

Note that most of the tests were only run once, thus the timings are only indicative. However, it is still possible to see that our implementations are more efficient also than `smatrixtdevdi` and approximately

⁶This is true in most cases for our problem but not in general.

h [a_{HO}]	Algorithm ¹	$\varepsilon/10^{-8}$	$\Delta E_0/10^{-6}$ [$\hbar\omega$]	t	h [a_{HO}]	Algorithm ¹	$\varepsilon/10^{-11}$	$\Delta E_0/10^{-8}$ [$\hbar\omega$]	t
10^{-2}	GSL	75.235	15.625	347 ms	10^{-3}	GSL [†]	-	-	> 10min
	Eigen	75.235	15.625	5.6 s		Eigen [‡]	-	-	-
	smatrixtdevd	75.235	15.625	1.6 s		smatrixtdevd [‡]	-	-	-
	smatrixtdevdi	75.235	15.625	~ 1 ms		smatrixtdevdi	75.228	15.620	13 ms
	FD (1)	75.235	15.625	~ 0 ms		FD (1)	75.227	15.625	~ 2 ms
	FD (2)	75.235	15.625	~ 0 ms		FD (2)	75.228	15.625	~ 2 ms
3×10^{-3}	GSL	2.0312	1.4063	37 s	5×10^{-4}	GSL [‡]	-	-	-
	Eigen	2.0312	1.4063	204 s		Eigen [‡]	-	-	-
	smatrixtdevd	2.0312	1.4064	63 s		smatrixtdevd [‡]	-	-	-
	smatrixtdevdi	2.0312	1.4064	~ 4 ms		smatrixtdevdi	9.4036	3.8697	26 ms
	FD (1)	2.0312	1.4063	~ 0 ms		FD (1)	9.4056	3.9062	~ 3 ms
	FD (2)	2.0312	1.4063	~ 1 ms		FD (2)	9.4044	3.9062	~ 4 ms

¹ We only report the names of the libraries, unless there is ambiguity.

[†] The algorithm was stopped.

[‡] No test was performed.

Table 3: Comparison between results and timings for the various tested subroutines/classes/algorithms.

equally accurate⁷, thus in what follows we shall only use these two.

To compare the accuracy and the efficiency of the finite difference algorithms against Numerov, for the three methods we tested the behaviour of the energy functional difference at convergence (calculated as average of this value after reaching stablization) and of the time used to perform a fixed number of self-consistent steps as functions of the mesh step h . The results are portrayed in Figs 11, 12 and 13. Note that also in this case the tests were only run once, thus the timings, especially when small, may be poorly accurate and/or affected by incidental slowdowns (nevertheless, it is still possible to discern an overall behaviour).

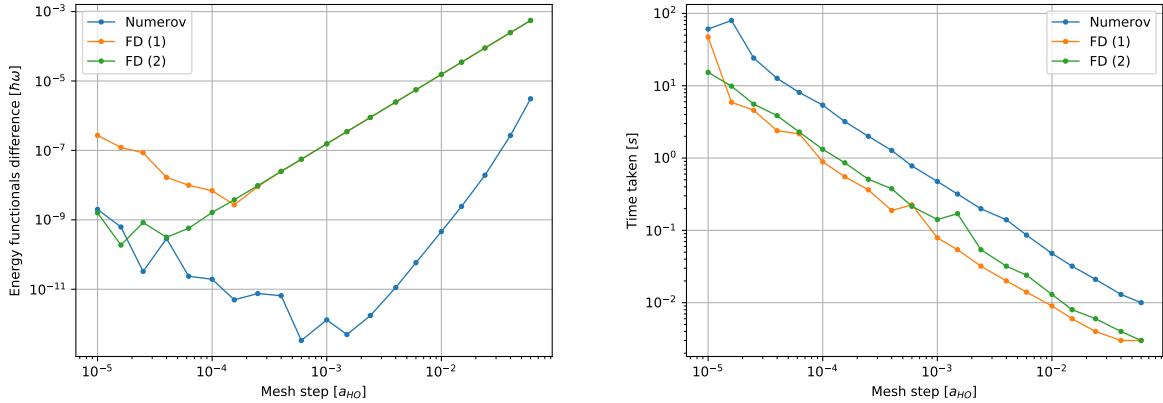


Figure 11: *Left*: Energy functionals difference as functions of h at convergence for $Na = 0.01$. *Right*: Time taken for 50 iterations for $Na = 0.01$ with $r_{\text{max}} = 6$.

The plots show that the Numerov algorithm can reach higher accuracy than the finite difference ones. In fact, as expected, the convergence accuracy of the finite difference algorithms seems to scale as h^2 for high h , whereas for the Numerov algorithm it scales as h^4 . At lower h , the error due to loss of numerical precision dominates and appears to be of the same magnitude for Numerov and FD (2) while more significant for FD (1). On the other side, the finite difference algorithm is in general more efficient of a factor of ~ 5 . These plots also allow to understand that, if we were to set a fixed threshold for the energy functionals difference, achievable for both algorithms, and choose a suitable mesh step to reach

⁷This, at least, for the ground state of the harmonic oscillator. In truth, we also tested `smatrixtdevdi` for the solution of the Gross-Pitaevskii equation, actually obtaining a behaviour of the energy functionals difference at convergence worse than our first implementation at low h .

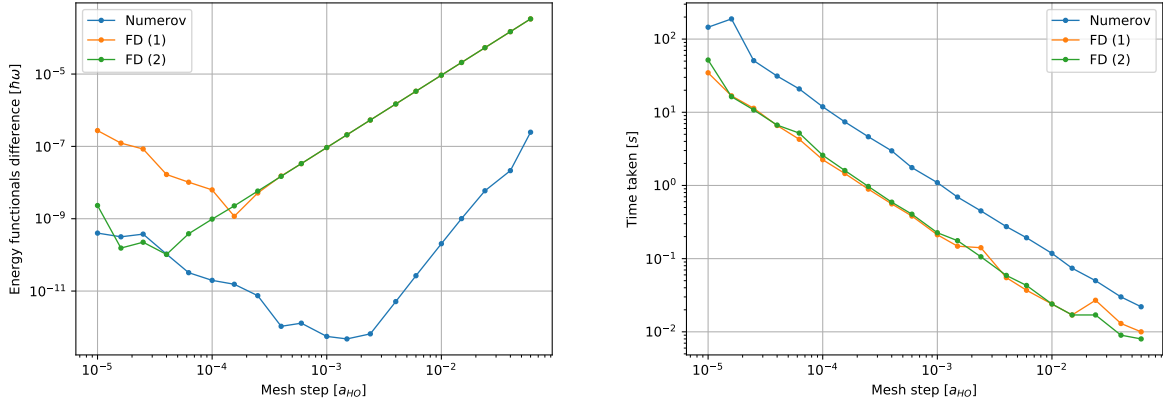


Figure 12: *Left*: Energy functionals difference as functions of h at convergence for $Na = 1$. *Right*: Time taken for 100 iterations for $Na = 1$ with $r_{\max} = 6$.

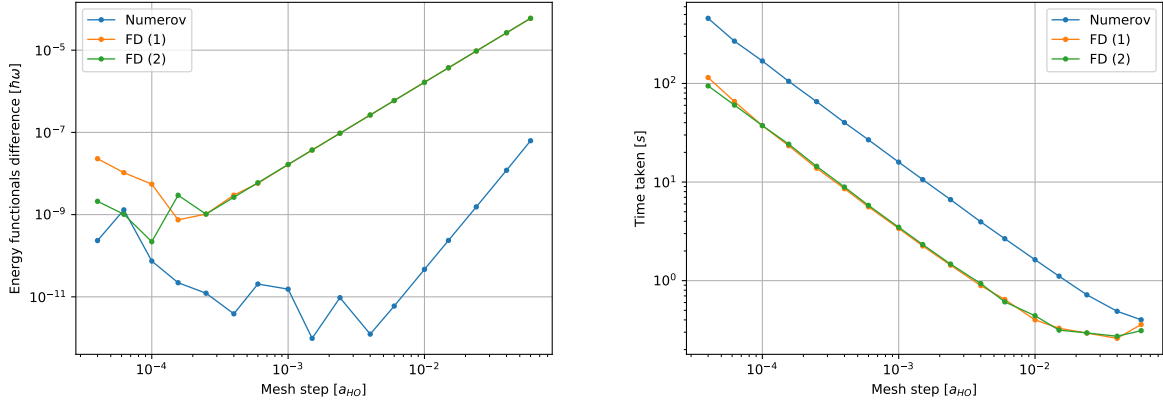


Figure 13: *Left*: Energy functionals difference as functions of h at convergence for $Na = 100$. *Right*: Time taken for 400 iterations for $Na = 100$ with $r_{\max} = 8$.

it, the Numerov algorithm would still be preferable as it would be more efficient. This is due to the fact that the number of steps needed to reach a given achievable energy functionals difference doesn't depend on the specific algorithm, but only on α . This fact is illustrated in Fig. 14, where we compare the convergence rate of Numerov and FD (2) for an arbitrary threshold. Both curves reach the threshold $E_t = 2 \times 10^{-9}$ at the same iteration, though Numerov (even if a higher thus faster h could still allow to reach the same threshold) takes ~ 0.58 s whereas FD (2) takes ~ 5.1 s.

On the contrary, if one were to set a threshold for the energy functionals difference achievable by both algorithms and also fix the value of h to be used by *both* algorithms, since the behaviour of $|E[\phi] - E_\mu[\phi]|$ only depends on α FD(1) and FD(2) would instead be preferable over Numerov, as they would take about a fifth of the time it would take to Numerov. This is easily understood once again looking at the plots on the right of Figs 11, 12 and 13.

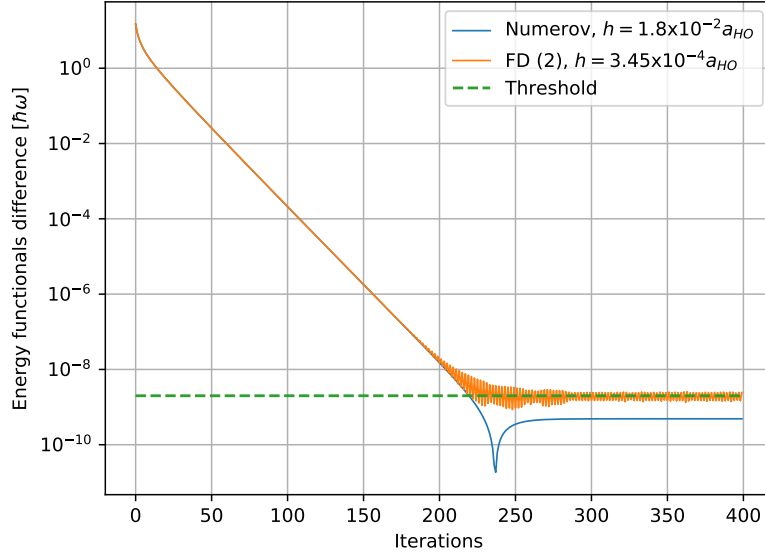


Figure 14: Comparison between convergence to an arbitrary threshold of the energy functional difference as a function of the number of self-consistent steps for Numerov and FD (2).

3.5 Point 5

Finally we study the behaviour of the equation and the self consistent procedure for negative Na . From a physical point of view, this means that we are considering an attractive potential rather than a repulsive one. We tested different values of Na using the Numerov algorithm, as it proved to be capable of reaching high accuracy in a rather short time.

We found that the system reaches an unstable state at approximately $Na = -0.575$. This value is the same obtained by Ruprecht *et al.* [2]. The instability of the system can be appreciated in Fig. 15, where we plot only some significant values of Na .

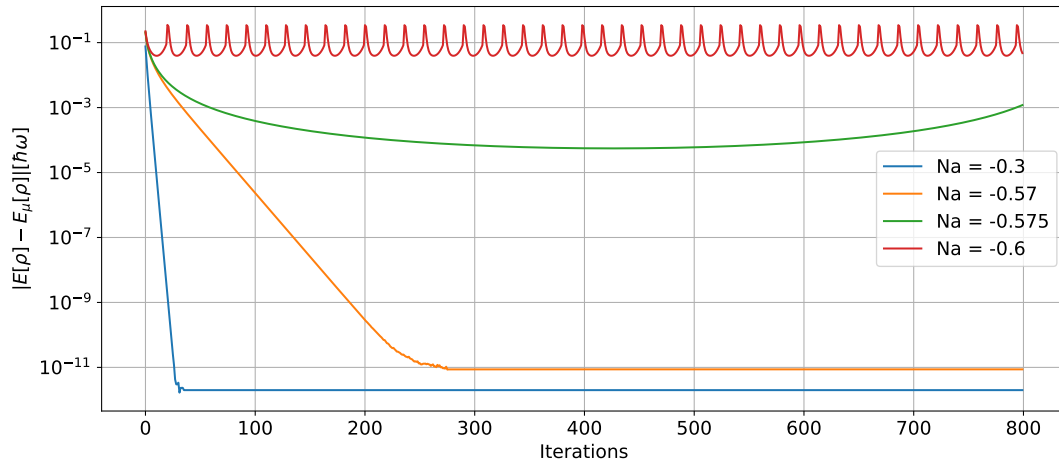


Figure 15: Comparison of behaviour of the single particle energy functionals differences as functions of the number of self-consistent steps for some negative values of Na .

We can notice that for $Na = -0.3$ and $Na = -0.57$ the difference in the single particle energy functionals $E[\rho]$ and $E_\mu[\rho]$ converges as for positive values of Na . What is interesting is the behaviour at $Na =$

-0.575 , as $|E[\rho] - E_\mu[\rho]|$ decreases though with a positive second derivative, reaches a minimum and increases again. The situation becomes dramatic beyond the value $Na = -0.575$, in fact, at $Na = -0.6$, the energy functionals difference oscillates around 10^{-1} . In Fig. 16 we show the difference between two even closer values of $N|a|$ for more iterations.

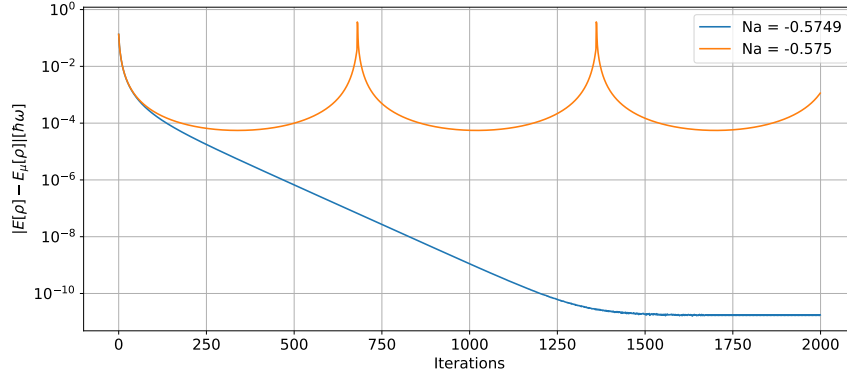


Figure 16: Comparison of behaviour of the energy functionals differences as functions of the number of self-consistent steps for $Na = -0.5749$ and $Na = -0.575$. Note that the frequency of oscillation of the $Na = -0.575$ curve is higher than that in Fig. 15 due to the usage of $\alpha = 1$ here and $\alpha = 0.8$ above.

There is a physical explanation for this instability. As already mentioned, negative values of Na correspond to an attractive interaction force, and due to this the density of particles at $r = 0$ tends to increase. Let us go back to the expression of the energy functional:

$$E[\rho] = T[\rho] + V_{\text{ext}}[\rho] + V_{\text{int}}[\rho] \quad (31)$$

When Na is negative, the interaction term $V_{\text{int}}[\rho]$ is also negative; the density at $r = 0$ then increases because this way the interaction energy $V_{\text{int}}[\rho]$ becomes large in modulus and this is favourable as it lowers the energy functional. This behaviour is opposed by the zero-point kinetic energy, which is able to stabilize the system and is represented by the kinetic term $T[\rho]$, which is often also called *quantum pressure*. When the central density is too high, the kinetic energy is no longer able to prevent the collapse of the gas. This implies that if the number of particles is too large (higher than a critical value N_{cr}), the gas collapses.

This collapse can be predicted from an analytical point of view as well. When we consider small (in modulus) values of Na , the functional $E[\rho]$ has a minimum and the system is therefore meta stable⁸. As instead, for a given a , when we consider a value of $N > N_{cr}$, $E[\rho]$ ceases to display a minimum and therefore the system is not stable.

We now proceed to show that the Gross-Pitaevskii equation admits the existence of meta stable states for values of N lower than a N_{cr} when the interaction potential is attractive and that they disappear for $N > N_{cr}$. Moreover we also obtain a rough theoretical estimate of the value of N_{cr} (or rather, of $N_{cr}a$).

In order to do so, we use a variational approach, as done by Dalfovo *et al.* [3]. As trial function we use a simple Gaussian multiplied by r , parametrised by the quantity w :

$$R(r) = \frac{2}{w^{3/2}\pi^{1/4}} r e^{-\frac{r^2}{2w^2}} \quad (32)$$

w represents the width of the Gaussian and makes physical sense only when it takes positive nonzero values. This trial wave function is a reasonably good for 2 main reasons: it is easy to manipulate from

⁸Later we shall explain explicitly why we talk about a meta stable state with an example.

an analytical point of view and it resembles the wave function that we obtain at the end of the self consistent algorithm (Fig. (18)). As usual, we calculate the energy functional corresponding to the trial wave function and minimize it with respect to w . The functional has the form

$$E(w) = \frac{3}{4} (w^{-2} + w^2) - (2\pi)^{-1/2} N |a| w^{-3} \quad (33)$$

We can interpret $E(w)$ as a function of w , but parametrized by N ($N|a|$). Fig. 17 features the behaviour of $E(w)$ for different values of $N|a|$.

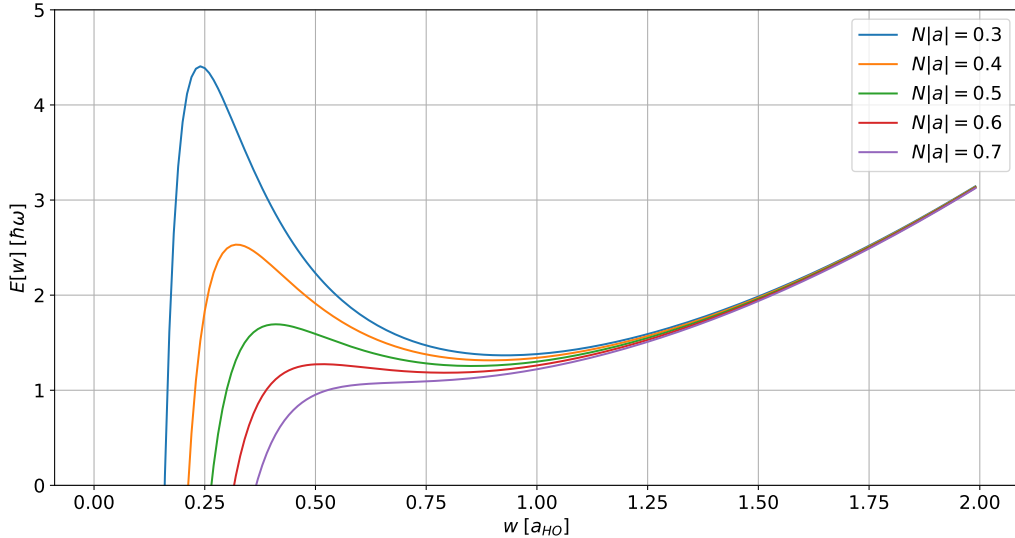


Figure 17: Plot of the energy $E(w)$ as function of w for different negative values of Na .

Fig. 17 allows to understand why we can talk about meta stable states. It is possible to notice that there is a local minimum when $N|a| \leq 0.6$, but $N|a| = 0.7$ displays no local minima. This would mean that the optimal value of w is 0, but as mentioned above this gives an nonphysical wave function.

As already mentioned, a meta stable state is associated with a local minimum of $E(w)$ and the gas collapses when this minimum disappears. This means that at the critical point the first and the second derivatives of $E(w)$ with respect to w vanish. This corresponds to the values $w_{cr} = 5^{-1/4}$ and $N_{cr}|a| = 2\sqrt{2\pi}/5^{5/4} \simeq 0.6705$, which is not extremely close to the value that we obtained numerically, but is of the same order. The accuracy of this result could increase considering more Gaussian functions and more adjustable parameters (like w), though this goes beyond the purpose of this section, which is to show why the Gross-Pitaevskii equation gives unstable solutions for large negative values of Na .

The fact that the system becomes unstable may be due to the fact that the Gross-Pitaevskii equation considers a dilute system and the interaction is approximated to the first order. When the density of particles becomes high, maybe higher order terms cannot be neglected thus this approximation fails.

Lastly, we point out that the energy functionals difference is a good parameter to determine the critical point. For example, one could only verify whether the wave functions or the respective potentials show any pathological behaviour by making a plot after a fixed large number of self consistent iterations. This, however, does not seem to be the case, as shown in Fig. 18, where we portray the wave functions and potentials obtained for various values of Na after 800 steps. Of course, we know that for $Na < -0.575$ the energy functionals difference fluctuates wildly and one single wave function is not representative for this oscillation, though here we assumed to only know the wave functions and the potentials.

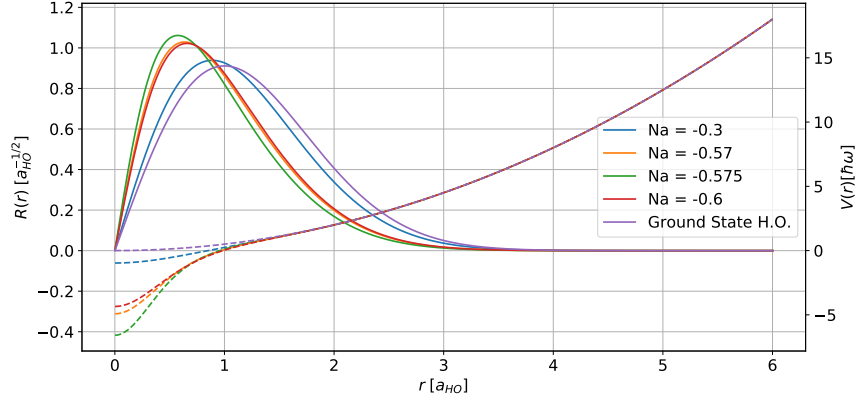


Figure 18: Comparison between wave functions and potentials after 800 self consistent steps for different negative values of Na . Note that the potential is referred to the y axis on the right.

In this plot we can notice that the wave functions have roughly the same form of the ground state of the harmonic oscillator, thus the usage of the aforementioned trial wave function for the estimation of N_{cr} is justified.

4 Conclusions

We solved numerically the Gross-Pitaevskii equation with an iterative procedure. We used an initial guess for the wave function, we solved the equation and we repeated this procedure by inserting the new wave function in the Hartree potential again. However, in order to reach converge we need to perform a mixing between the previous Hartree potential and the new one. This procedure is not valid only for the Gross-Pitaevskii equation, but can be easily adapted to other self-consistent equations, as Hartree-Fock equations.

We have studied one single iteration of the algorithm. The new wave function is close to the ground state of the harmonic oscillator for small values of α and Na , while for bigger values it begins shifting towards larger values of r . Lastly we have observed that for large enough values of α and Na , the wave function changes behaviour significantly close to the origin.

Later we have found the best parameter α in order to reach convergence for 5 different values of Na . We obtained that for $Na = 0.01, 0.1$ the best α is equal to 1, i.e. no mixing is needed. For the other values of Na we need a smaller α , which implies that the convergence time is longer. Moreover we found that the wave function is significantly different from the ground state of the harmonic oscillator for high Na .

Then we tested a different algorithm to integrate numerically one iteration of the Gross-Pitaevskii equation. We found that, if we fix h , independently on Na and α , the finite difference algorithm is preferable over the Numerov algorithm because it is faster, though it can't reach the accuracy of the Numerov algorithm. On the contrary, if we choose the optimal value of h for a given energy functionals difference threshold, the Numerov algorithm is the best algorithm between the two.

Finally we inspected what happens for negative values of a , i.e. the force is attractive rather than repulsive. For small $N|a|$, the algorithm converges, while for high $N|a|$, the system is unstable and the algorithm does not converge. This is due to the fact that, for low $N|a|$, the system is in a meta stable state and there is a local minimum in the energy functional. Above a critical value $N_{cr}|a|$, this local minimum disappears. The critical value that we obtained is $Na \simeq -0.575$.

Appendix A Code and data depository

The data were simulated using C++, while the plots and the data analysis were made in Python. The code written for simulating the data of this report is available at the link https://github.com/FrancescoSlongo/Computational-Physics---Trento/tree/master/Project_3.

References

- [1] F. Pederiva. *Mean Field Calculations for Bosons; Lecture slides for the Advanced Computational Physics Course*. University of Trento, 2020.
- [2] Ruprecht, P. A., M. J. Holland, K. Burnett, and M. Edwards, 1995, Phys. Rev. A 51, 4704
- [3] F. Dalfovo, S. Giorgini, Lev P. Pitaevskii, S. Stringari, Rev. Mod. Phys. 71, 463 (1999)